Supporting Information

Top-Down Fabrication of Hierarchical Nanocubes on Nanosheets Composite for High-Rate Lithium Storage

Jian-Ping Zhang, Xue-Yan Wu,* Xiao Wei, Shu-Mao Xu, Chao Ma, Mou-Hai Shu,* Kai-Xue Wang, and Jie-Sheng Chen

School of Chemistry and Chemical Engineering, Shanghai Jiao Tong University, Shanghai 200240, China.

* To whom correspondence should be addressed. E-mail: xueyanwu@sjtu.edu.cn (XYW); mhshu@sjtu.edu.cn (MHS)

This file includes Figure S1-S9 and Table S1.

Figure S1.

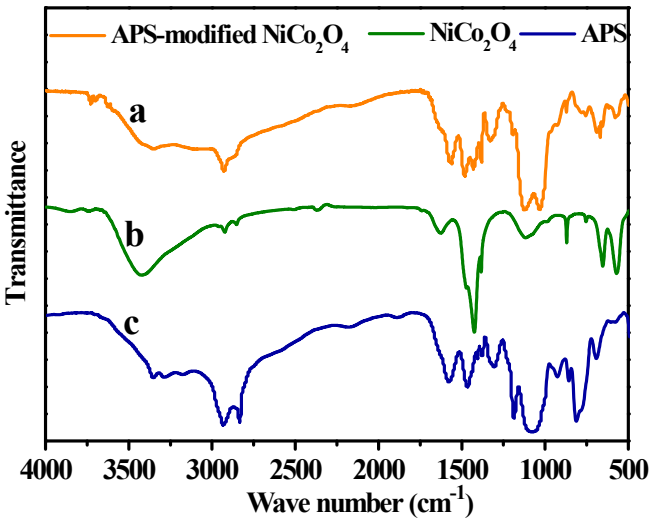

Figure S1. FTIR spectra of (a) APS-modified $NiCo_2O_4$ spheres, (b) pure $NiCo_2O_4$ spheres and (c) pure APS.

Figure S2.

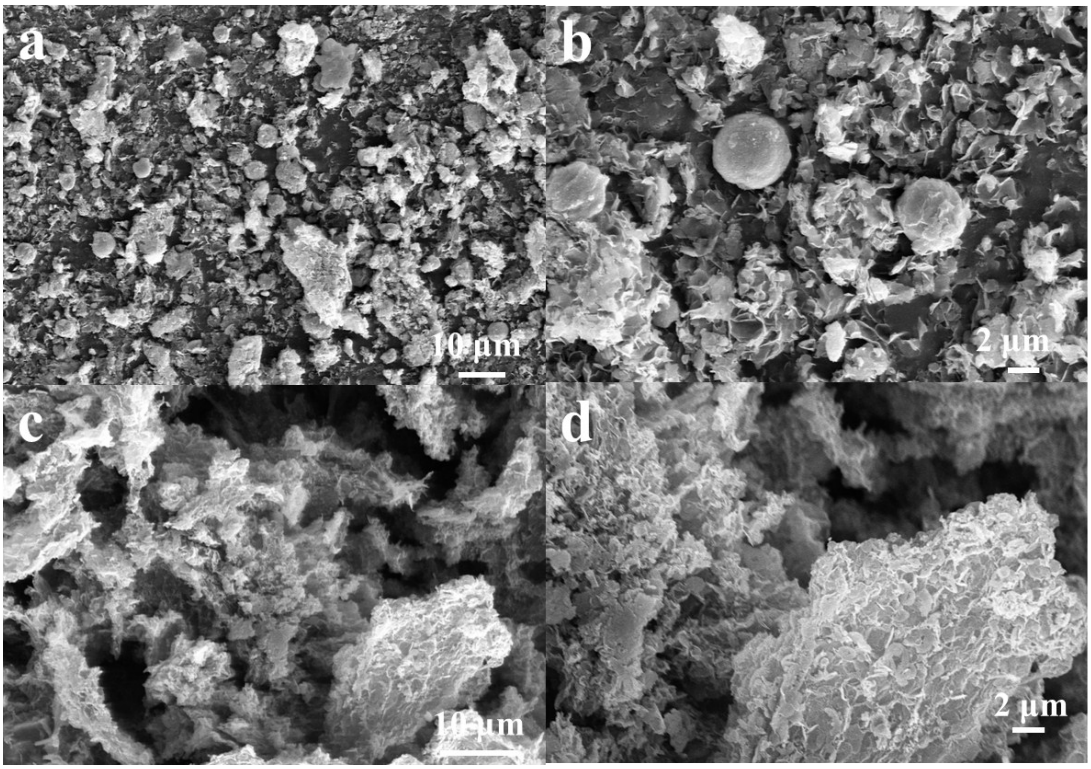

Figure S2. Low- and high-magnification SEM images of composites with (a,b) a small amount of GO and (c,d) excessive GO.

Figure S3.

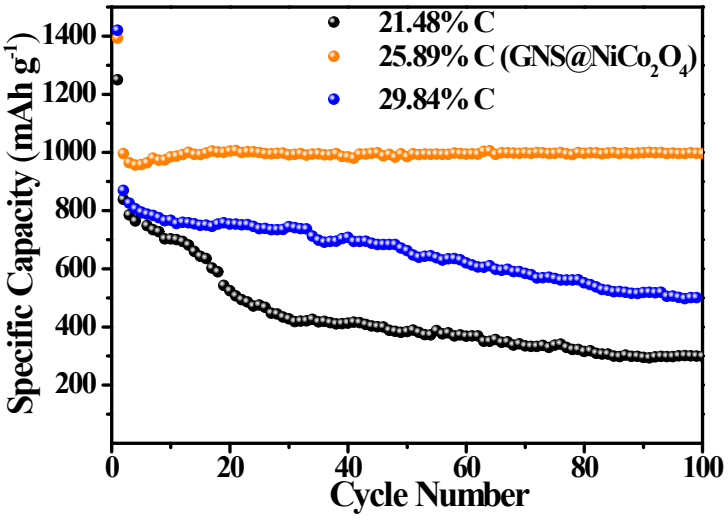

Figure S3. Cycling performance of the GNS@$NiCo_2O_4$ composites with different carbon contents cycled at a current density of 100 mA g^{-1} for 100 cycles.

Figure S4.

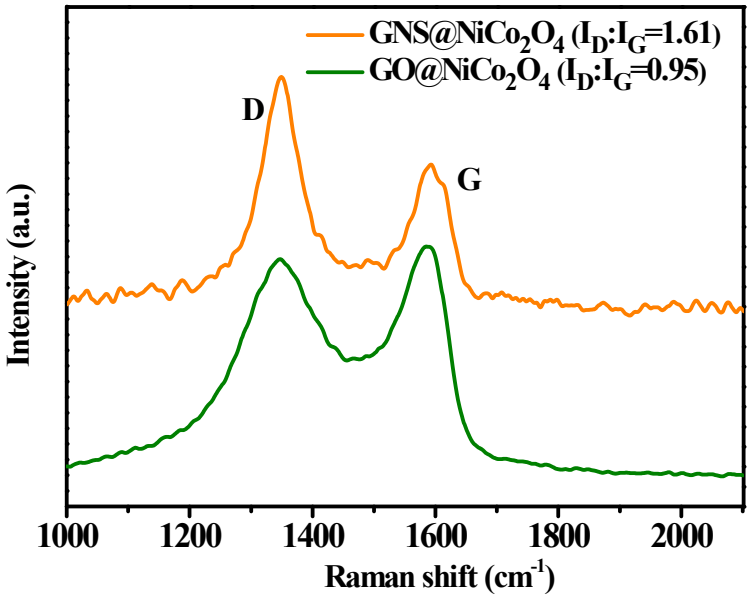

Figure S4. Raman spectra of GNS@$NiCo_2O_4$ and GO@$NiCo_2O_4$.

Figure S5.

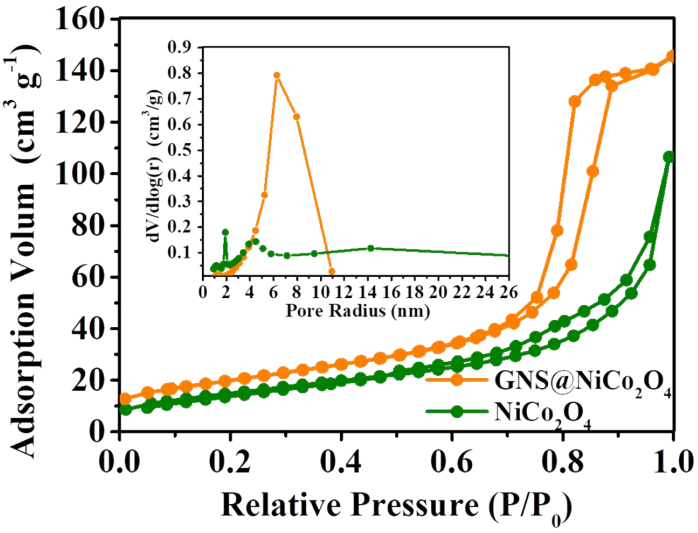

Figure S5. Nitrogen adsorption-desorption isotherms and BJH pore size distributions of $NiCo_2O_4$ spheres and GNS@$NiCo_2O_4$ composites.

Figure S6.

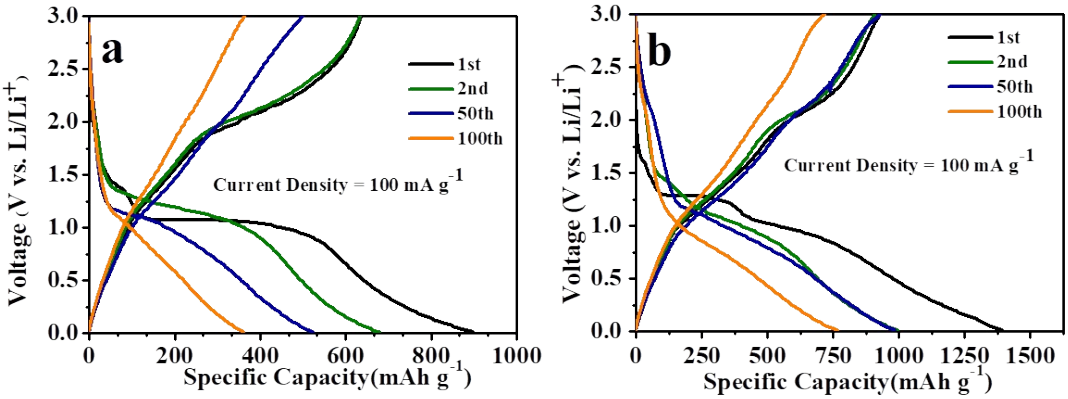

Figure S6. Galvanostatic discharge-charge voltage profiles of (a) $NiCo_2O_4$ spheres and (b) GNS@$NiCo_2O_4$ composites at a current density of 100 mA g^{-1}.

Figure S7.

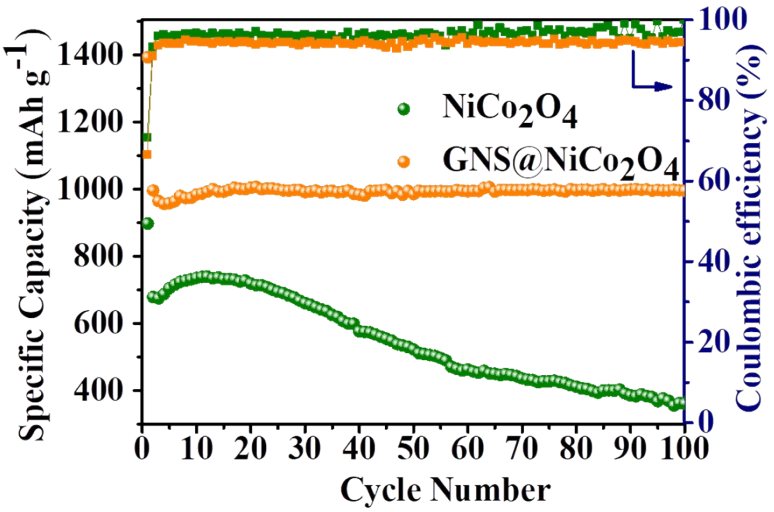

Figure S7. The comparative cycling performance of the GNS@$NiCo_2O_4$ composites and $NiCo_2O_4$ spheres at a current density of 100 mA g^{-1} for 100 cycles.

Figure S8.

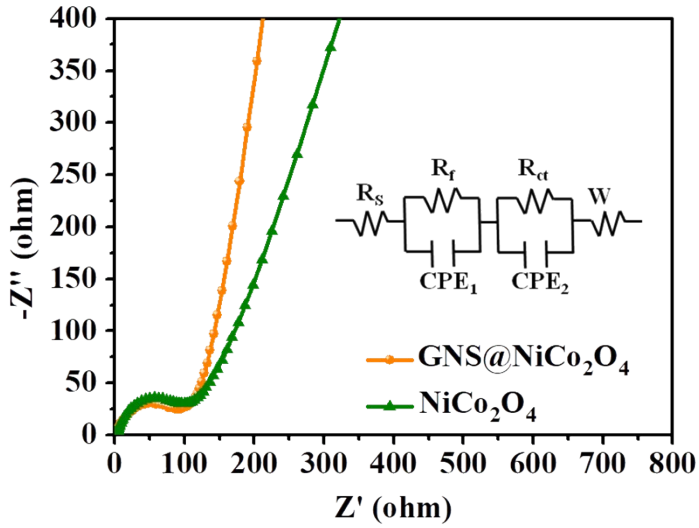

Figure S8. The EIS spectras of GNS@$NiCo_2O_4$ composites and $NiCo_2O_4$ spheres before cycles at a frequency range of 10^5 Hz to 0.1 Hz.

Figure S9

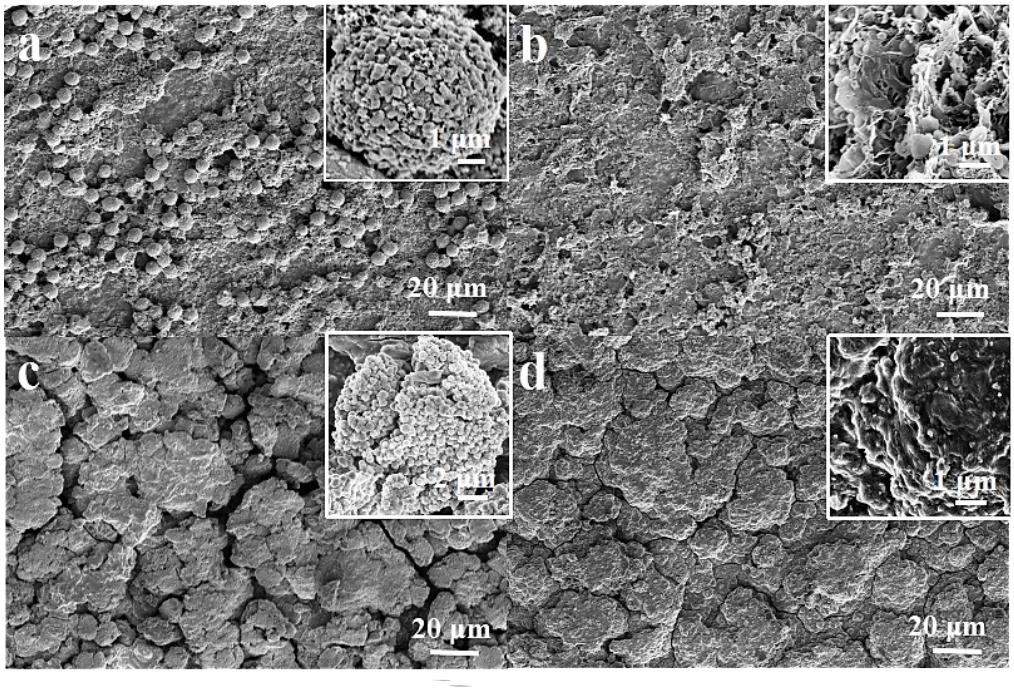

Figure S9. SEM images of the electrodes on copper foil (a,b) before and (c,d) after discharged/charged at a current density of 500 mA g^{-1} for 200 cycles. (a,c) bare $NiCo_2O_4$ spheres; (b,d) GNS@$NiCo_2O_4$ composites.

Table S1. Comparing with $NiCo_2O_4$ materials or its composite with conductive matrix as anode for LIB reported in previous literature

Materials	**Current Density ($mA\ g^{-1}$)**	**Reversible capacity ($mA\ h^{-1}$) / cycle number**	**Ref.**
$NiCo_2O_4$-C nanorods	500	863/200th	[1]
$NiCo_2O_4$@C/carbon cloth composite	500	807/100th	[2]
$NiCo_2O_4$ flower-like structure	100	939/60th	[3]
$NiCo_2O_4$ dried plum-like spheres	100	801/50th	[4]
$NiCo_2O_4$ nanoplates on RGO	100	816/70th	[5]
$NiCo_2O_4$ nanorods	100	856/100th	[6]
This work	500	1024/200th	
	100	998/100th	

References

1 L. Peng, H. Zhang, Y. Bai, J. Yang and Y. Wang, *J. Mater. Chem. A*, 2015, **3**, 22094-22101.

2 K. Wang, Y. Huang, M. Wang, M. Yu, Y. Zhu and J. Wu, *Carbon*, 2017, **125**, 375-383.

3 L. Li, Y. Cheah, Y. Ko, P. Teh, G. Wee, C. Wong, S. Peng and M. Srinivasan, *J. Mater. Chem. A,* 2013, **1**, 10935-10941.

4 T. Li, X. Li, Z. Wang, H. Guo and Y. Li, *J. Mater. Chem. A,* 2015, **3**, 11970-11975.

5 Y. Chen, M. Zhuo, J. Deng, Z. Xu, Q. Li and T. Wang, *J. Mater. Chem. A,* 2014, **2**, 4449-4456.

6 F. Fu, J. Li, Y. Yao, X. Qin, Y. Dou, H. Wang, J. Tsui, K. Y. Chan and M. Shao, *ACS Appl. Mater. Interfaces,* 2017, **9**, 16194-16201.